

A Simple Model of Flow-Induced Crystallization Memory

Andrzej Ziabicki* and Giovanni Carlo Alfonso°

*) Polish Academy of Sciences, Institute of Fundamental Technological Research,
21 Swietokrzyska St., Warsaw, Poland

°) Institute of Chemistry and Industrial Chemistry, University of Genoa,
via Dodecaneso 31, Genoa, Italy

Summary: Flow induced crystallization of polymer systems exhibits strong memory effects. Crystalline structures gradually change when the flow is switched off and the polymer is relaxed prior to crystallization. A simple model based on the multidimensional theory of crystal nucleation^[1] is proposed. Steady, potential flow applied to a polymer fluid above melting temperature ($T_p > T_m$) results in molecular orientation of crystallizing units. The flow controls formation of molecular clusters which convert into athermal nuclei when the system is cooled down to crystallization temperature, $T_c < T_m$. Orientation effects gradually disappear when the melt is relaxed above T_m in the absence of flow or stress.

1. Introduction

A few years ago[2-3] we have discussed «structural memory» of a crystallizable polymer subjected to prolonged heating above melting temperature, T_m . Melt structure was discussed in terms of distribution of molecular clusters, some of which became spontaneously growing **athermal nuclei** when cooled down below T_m . More recently, several authors observed effects of molecular orientation introduced into the melt prior to crystallization on microscopic structure of the subsequently formed crystals^[4-7]. This «orientation memory» gradually disappeared when orientation was followed by heating of the melt in quiescent conditions.

We will discuss a simple model of flow-induced «orientation memory». Orientation produced by elongational flow is partly relaxed at a temperature $T_R > T_m$ for a period t_R . The system is rapidly cooled and crystallized at the temperature $T_c < T_m$. Oriented structures observed in crystallized samples are indicative of the presence of oriented clusters which survived relaxation and were converted into athermal nuclei.

The model is too simplified to describe experimental data^[4-7] quantitatively. Nevertheless, based on sound thermodynamic principles, the model reflects important mechanisms of oriented crystallization and explains physical nature of the observed phenomena.

2. Aggregation of asymmetric molecular units

We are considering cylindrical clusters with radius r and length, l , composed of g single kinetic elements. The latter are rodlike particles, with a volume v_0 . The bulk free energy of a cluster is proportional to cluster volume, $v \approx g v_0$, and surface energy is controlled by two different interface tensions, one on the front (σ_e) another one on the side surface of the cluster (σ_s). For the sake of simplicity, we consider clusters with a constant, thermodynamically optimum shape

$$(1/r) = \text{const.} = (1/r)_{\min} = \frac{2\sigma_e}{\sigma_s} \quad (1)$$

corresponding to minimum surface energy. Free energy of formation of a cluster composed of g kinetic elements, ΔF ,

$$\Delta F(g) = \Delta F_{\text{bulk}} + \Delta F_{\text{surf}} = (g - 1) v_0 \Delta f + 3(g^{2/3} - 1) v_0^{2/3} (2\pi\sigma_e\sigma_s^2)^{1/3} \quad (2)$$

is expressible through a single size variable (reduced cluster volume), $g = v/v_0$ (density changes are neglected for simplicity). Δf is bulk free energy density of cluster formation.

We are considering aggregation of axially symmetric molecular units in a steady, isochoric elongational flow characterized with velocity gradient q^*

$$\nabla V = q^* \begin{bmatrix} -\frac{1}{2} & 0 & 0 \\ 0 & -\frac{1}{2} & 0 \\ 0 & 0 & 1 \end{bmatrix} \quad (3)$$

The reason why *elongational*, rather than *shear* flow is considered, is related to thermodynamics. Interaction of asymmetric particles with a potential (e.g. elongational) flow contributes well defined thermodynamic potential. On the other hand, the behavior of particles in any rotational flow (including shear flow) can hardly be discussed in terms of equilibrium thermodynamics^[8].

Aggregation of asymmetric, orientable particles in a flow field depends on *orientation* of single kinetic units and of the resulting clusters. Since elongational flow is uniaxial, and symmetry of all units is cylindrical, orientation can be characterized with a single variable, ϑ ,

angle between particle axis and axis of the flow.

Orientation dependent bulk free energy density includes, in addition to the reference value, Δf_0 , two flow related terms^[1]

$$\Delta f(\vartheta) = \Delta f_0 + \Delta u(\vartheta) - \frac{kT}{v_0} \ln[4\pi\rho(\vartheta)] \quad (4)$$

The first extra term describes the change of *potential energy of interaction* of single kinetic units and clusters *with the flow field*. The second term, related to orientation distribution of aggregating units, $\rho(\vartheta)$, provides change of *mixing entropy* of the mother phase. Δf_0 denotes free energy density in the absence of flow. In steady elongational flow the difference of interaction potential density between a crystallizing molecule and the growing cluster assumes the form^[8]

$$\Delta u(\vartheta) = \frac{U_{cl}(\vartheta)}{g v_0} - \frac{U_1(\vartheta)}{v_0} = \frac{-3kTq \cos^2 \vartheta}{4v_0} \left[\frac{R_{cl}}{g \cdot D_{rot,cl}} - \frac{R_1}{D_{rot,1}} \right] = \frac{kTH \cos^2 \vartheta}{v_0} (C - 1) \quad (5)$$

where

$$C = \frac{R_{cl} D_{rot,1}}{g R_1 D_{rot,cl}} \quad (6)$$

is a dimensionless constant of the order of unity. R denotes shape constants, and D_{rot} – rotational diffusion coefficients, both characteristics different for clusters and for aggregating kinetic units. The negative parameter

$$H = \frac{-3q \cdot R_1}{4D_{rot,1}} \quad (7)$$

characterizes intensity of potential interactions with the flow field.

In steady elongational flow, orientation of rodlike particles is subject to equilibrium, Boltzmann-type distribution

$$\rho_{eq}(\vartheta) = \text{const.} \exp \left[\frac{-U_1(\vartheta)}{kT} \right] = \frac{1}{Z} \exp[-H \cos^2 \vartheta] \quad (8)$$

where

$$Z(H) = \int_0^{\pi} \exp[-H \cos^2 \vartheta] \sin \vartheta \, d\vartheta$$

$Z(H)$ is configurational integral. Figure 1 presents equilibrium distribution $\rho_{eq}(\vartheta)$ for several field intensities. Maximum density corresponds to $\vartheta = 0$, minimum to $\vartheta = \pi/2$.

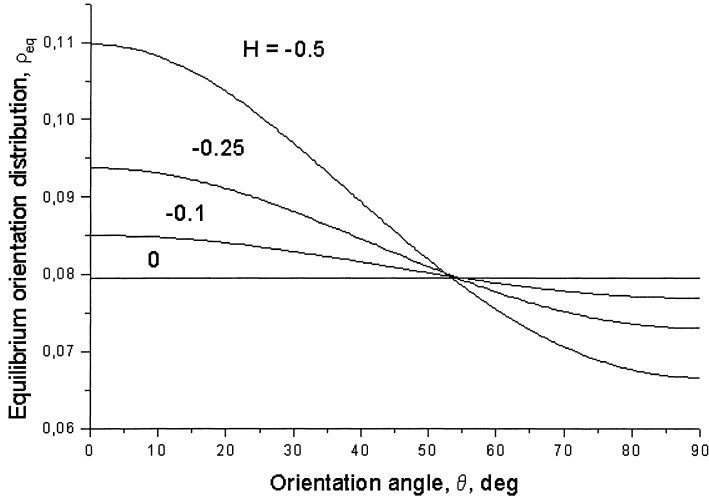


Figure 1. Equilibrium orientation distribution of rodlike kinetic units, $\rho_{eq}(\vartheta)$, calculated from Eq.(8) for a melt subjected to steady elongational flow. $T_p = 510$ K Field intensity, H , indicated.

With equilibrium orientation distribution, bulk free energy of aggregation assumes the form

$$\Delta f(\vartheta) = \Delta f_0 + \frac{kT}{v_0} \left[C \cdot H \cos^2 \vartheta + \ln \left(\frac{Z(H)}{4\pi} \right) \right] \quad (9)$$

and reduces to Δf_0 in stationary equilibrium ($H = 0$, $Z = 4\pi$). For the sake of simplicity, we will assume $C = 1$, which is equivalent to linear rescaling of the parameter H . When the flow is switched off ($\Delta u = 0$), free energy of the *transient state* is controlled by non-equilibrium, time-dependent distribution $p(\vartheta, t)$

$$\Delta f(\vartheta, t) = \Delta f_0 - \frac{kT}{v_0} \ln[4\pi\rho(\vartheta, t)] \quad (10)$$

The fact that orientation affects bulk free energy of aggregation has far going consequences. In the conditions of steady flow (steady orientation distribution) the *equilibrium transition (aggregation) temperature* depends on flow intensity, H , and also on *orientation of individual clusters (crystals)*^[1, 9].

Equilibrium melting temperature

$$T_{m,eq}(\vartheta; H) = T_{m0} \frac{\Delta h_0}{\Delta h_0 + \frac{kT_{m0}}{v_0} \left[C \cdot H(T_m) \cos^2 \vartheta + \ln \frac{Z(T_m)}{4\pi} \right]} \cong \quad (11)$$

$$\cong T_{m0} \frac{1}{1 + \frac{kT_{m0}}{\Delta h_0 v_0} \left[H(T_m) \cos^2 \vartheta + \ln \frac{Z(T_m)}{4\pi} \right]}$$

behaves in a way similar to orientation distribution, ρ_{eq} : higher melting temperatures correspond to small orientation angles, lower – to large angles. This is evident in Figure 2. Consider a system with quiescent equilibrium melting temperature ($H = 0$), $T_{m0} = 481$ K. Application of a relatively weak flow ($H = -0.25$), elevates T_m to 507.3 K for parallel oriented clusters ($\vartheta = 0$), and for perpendicular clusters ($\vartheta = \pi/2$) suppresses T_m below the reference level to 468.2 K.

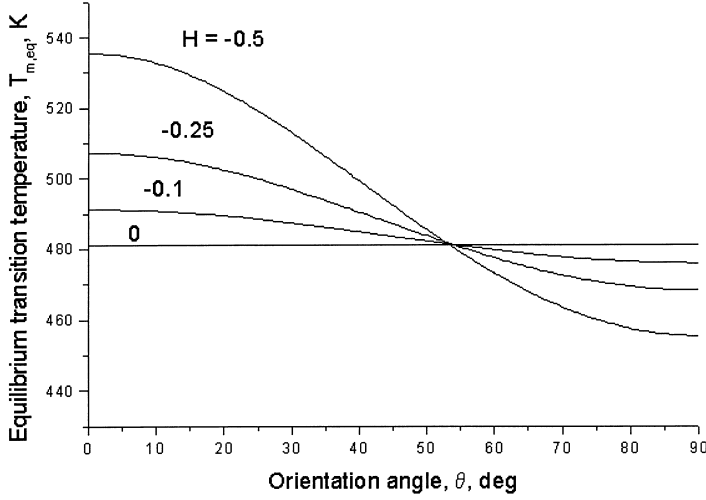


Figure 2. Equilibrium transition temperature, $T_{m,eq}(\vartheta)$, calculated from Eq.(11) for a polymer melt subjected to steady elongational flow. Field intensity, H , indicated.

When the flow is switched off, transient, relaxing orientation $\rho(\vartheta, t)$ characterizes *critical temperature for the onset of the transition*

$$T_m(\vartheta, t) = T_{m0} \frac{1}{1 - \frac{kT_{m0}}{\Delta h_0 v_0} \ln[4\pi\rho(\vartheta, t)]} \quad (12)$$

The distribution of clusters defined as a normalized density in the configurational space of cluster sizes and orientations, $w(g, \vartheta)$, is determined by the Fokker-Planck equation^[1]

$$\frac{\partial w}{\partial t} - \frac{\partial}{\partial g} \left[D_{gr} \left(\frac{\partial w}{\partial g} + \frac{w}{kT} \frac{\partial \Delta F}{\partial g} \right) \right] - \frac{1}{\sin \vartheta} \frac{\partial}{\partial \vartheta} \left[\sin \vartheta D_{rot} \left(\frac{\partial w}{\partial \vartheta} + \frac{w}{kT} \frac{\partial \Delta F}{\partial \vartheta} \right) \right] = 0 \quad (13)$$

where D_{gr} and D_{rot} denote, respectively, growth-, and rotational diffusion coefficients.

Above the melting temperature all clusters, however large, are unstable and do not grow to crystal dimensions. When the system is cooled down below T_m , some clusters become thermodynamically unstable and convert into spontaneously growing *athermal nuclei*. The

number of athermal nuclei active in the supercooled system ($T_c < T_m$) is controlled by cluster distribution, $w(g, \vartheta)$, and depends on the flow and relaxation conditions

$$N_{\text{ath}}(T_c, t) = 2\pi N_{\text{tot}} \int_0^\pi \sin \vartheta \, d\vartheta \int_{g^*}^\infty w(g, \vartheta, t) \, dg \quad (14)$$

N_{tot} is total number (concentration) of kinetic units in the system. The lower integration limit in Eq.(14), is critical cluster size, g^* , controlled by bulk free energy

$$g^*(T_c) = \frac{16\pi\sigma_e\sigma_s^2}{v_0[-\Delta f(T_c)]^3} = g_0^*(T_c) \left[\frac{\Delta f_0(T_c)}{\Delta f(T_c, \vartheta)} \right]^3 \quad (15)$$

Equilibrium orientation distribution in the conditions of steady flow, $\rho_{\text{eq}}(\vartheta; H)$ induces orientation dependent critical cluster size, effective on cooling down to crystallization temperature, T_c

$$g^*(\vartheta; H, T_c) = g_0^*(T_c) \left[\frac{\Delta f_0(T_c)}{\Delta f_0(T_c) + \left[H \cos^2 \vartheta + \ln\left(\frac{Z}{4\pi}\right) \right]} \right]^3 \quad (16)$$

When the flow is switched off, but orientation distribution is not random, g^* is controlled by transient orientation distribution, $\rho(\vartheta, t)$

$$g^*(\vartheta, t, T_c) = g_0^*(T_c) \left[\frac{\Delta f_0(T_c)}{\Delta f_0(T_c) - \frac{kT_c}{v_0} \ln[4\pi\rho(\vartheta, t)]} \right]^3 \quad (17)$$

$g^*(\vartheta)$ behaves in a way opposite to orientation distribution, or melting temperature: smaller critical cluster sizes correspond to small orientation angles, higher – to large angles (Figure 3). Relaxation in the absence of flow leads to gradual equalization of $g^*(\vartheta)$ values which asymptotically reach g_0^* .

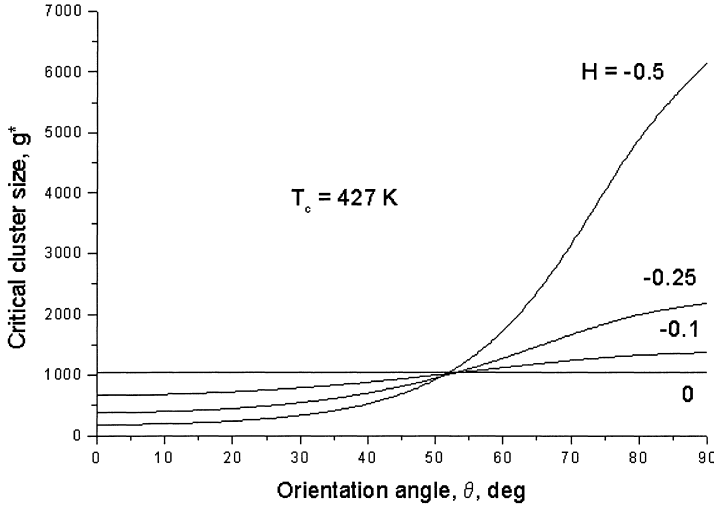


Figure 3. Critical cluster size, $g^*(\theta)$, calculated from Eq.(16) for a polymer melt subjected to steady elongational flow. Field intensity, H , indicated.

The highest concentration of nuclei and the highest rate of nucleation correspond to orientations close to $\vartheta = 0$. Crystallization on oriented nuclei produces oriented crystals. What controls nucleation is a fraction of nuclei contained in a narrow range of angles, $\vartheta \in (0, \delta\vartheta)$.

$$\Delta N_{\text{ath}}(T_c, t, \delta\vartheta) = 2\pi N_{\text{tot}} \int_0^{\delta\vartheta} \sin \vartheta \, d\vartheta \int_{g^*}^{\infty} w(g, \vartheta, t) \, dg \quad (18)$$

The density of effective athermal nuclei rapidly decreases with increasing orientation angle, ϑ . For the example considered it was found, that $\Delta N_{\text{ath}}(\delta\vartheta)$ practically levels off at $\delta\vartheta = 5 - 10^\circ$. Athermal nuclei with orientations $\vartheta > 10^\circ$ can thus be neglected.

In the following sections we will discuss changes in cluster distribution in the individual steps of the orientation and relaxation process, and the related concentration of athermal nuclei .

3. The Process

Thermomechanical history of the system includes:

- i. Heating of the sample to a temperature higher than melting temperature, $T_p > T_m$,

- ii. Application of elongational flow with an intensity H ,
- iii. Relaxation in quiescent conditions at a temperature higher than maximum critical temperature, $T_R > T_{m,max}$, for a period of t_R ,
- iv. Cooling down and crystallization in a subcritical temperature, $T_c < T_{m,min}$.

$T_{m,max} = T_m(\vartheta = 0)$, and $T_{m,min} = T_m(\vartheta = \pi/2)$ denote maximum and minimum melting temperature in an oriented system. The history of temperature and flow is presented schematically in Figure 4.

3.1. Heating

The sample is heated to a temperature T_p in the absence of stress. Equilibrium cluster size distribution, independent of orientation, is developed

$$w_{eq,0}(g; T_p) = \frac{\exp[-\Delta F_0(g, T_p) / kT_p]}{4\pi \int_1^{\infty} \exp[-\Delta F_0(g, T_p) / kT_p] dg} \quad (19)$$

Orientation distribution is random, and equilibrium cluster density, $w_{eq,0}(g)$ monotonically decreases with cluster size, g . In a superheated melt ($T_p > T_m$) all clusters, however large, are unstable and unable to grow spontaneously.

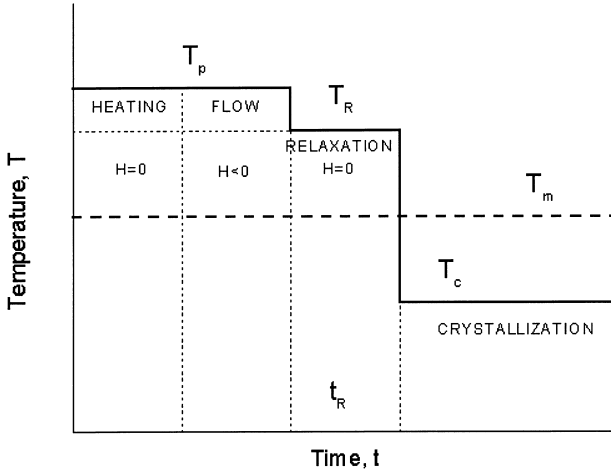


Figure 4. Temperature history in the process of orientation, relaxation, and crystallization (schematic).

3.2. Flow orientation

In the melt subjected to steady isothermal flow (T_p , H) another equilibrium distribution of single kinetic units and clusters is developed. Equilibrium distribution of single kinetic units, $\rho_{eq}(\vartheta; H)$ assumes the form indicated in Eq.(8)

The equilibrium distribution of clusters results from Eq.(13) combined with Eqs.(2) and (9).

For $C \approx 1$

$$\begin{aligned}
 w_{eq}(g, \vartheta) &= \text{const.} \exp \left[\frac{-\Delta F(g, \vartheta)}{kT_p} \right] \cong \\
 &\cong \text{const.} \exp \left[\frac{-\Delta F_0(g)}{kT_p} + (g-1) \left(H \cos^2 \vartheta + \ln \frac{Z(H)}{4\pi} \right) \right]
 \end{aligned} \tag{20}$$

where $\Delta F_0(g, T_p)$ is free energy of cluster formation in quiescent conditions.

When the system is rapidly transferred to a lower (crystallization) temperature, $T_c < T_{m, \max}$, some clusters (first of all, those oriented parallel to flow axis) become stable and contribute to crystallization as athermal nuclei.

Figure 5 presents orientation dependent distribution of critical clusters, $w_{eq} [\vartheta, g^*(\vartheta)]$, in steady elongational flow. Random distribution corresponding to a quiescent melt ($H = 0$) is dramatically changed in flow conditions. The density of parallel oriented clusters is increased, and that of perpendicular clusters reduced, by many orders of magnitude.

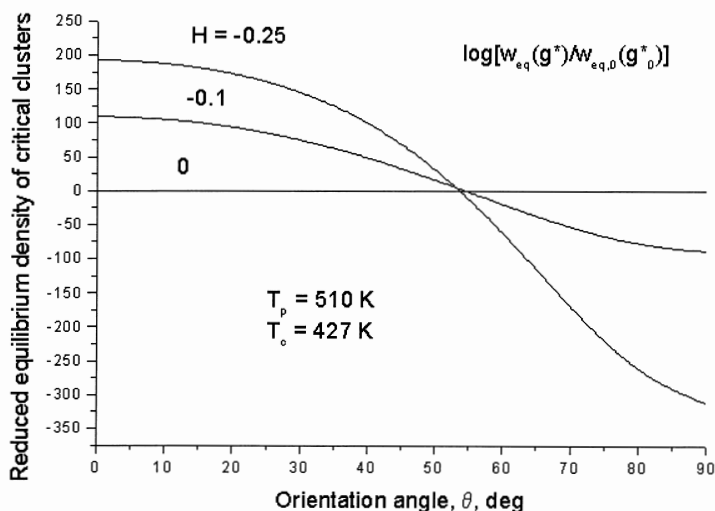


Figure 5. Reduced equilibrium density of critical clusters, $w_{eq}[(\vartheta, g^*(\vartheta))]$ created in steady elongational flow. Flow intensities, H , indicated.

In Figure 6 equilibrium cluster distributions, $w_{eq}(g)$, for a superheated melt subjected to steady flow ($H = -0.25$) is shown. The solid lines represent distributions for selected orientation angles, and solid circles – critical cluster sizes related to crystallization temperature, $T_c = 427$ K. Dashed line and open circles refer to an unoriented system ($H = 0$).

The measure of flow effects on crystallization is the number of athermal nuclei effective at the crystallization temperature, T_c . The number of such clusters is controlled by cluster distribution and the critical cluster size, g^* , providing lower integration limit in Eqs. (14) and (18). It is evident in Figure 6 that g^* dramatically increases with orientation angle, thus reducing the integration range and the number of effective nuclei. In the example considered in Figure 6, the reference (unoriented) critical cluster size, g_0^* is 1050. In the relatively weak flow field ($H=-0.25$), parallel clusters are stable already at $g = 375$, but perpendicular clusters

require $g = 2174$. The number of parallel oriented nuclei is enhanced by flow, both, via reduction of critical size, and by the increase in cluster density. Detailed analysis of the data shows that, within 10° around the flow direction, concentration of critical clusters drops below 1% of the maximum value. Consequently, effective nucleation (and crystallization) is confined to crystals nearly parallel to flow axis.

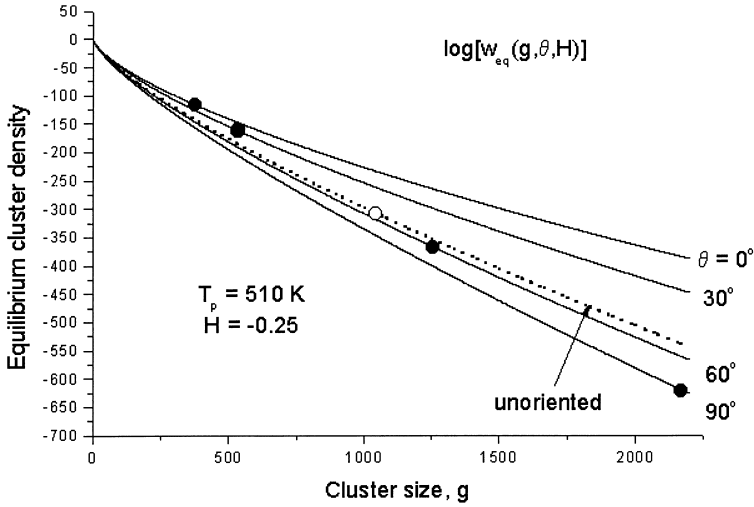


Figure 6. Equilibrium cluster density, $w_{eq}(g)$, in a superheated melt subjected to steady elongational flow ($H = -0.25$). Solid lines correspond to selected orientation angles (indicated). Solid circles indicate critical cluster sizes, g^* , for individual distributions. Dashed line and open circle describe unoriented system ($H = 0$).

3.3. Relaxation

When the flow is switched off, and the sample is held in a temperature higher than the critical one, orientation distributions relax from the initial, flow controlled, level to a new equilibrium, corresponding to temperature T_R and quiescent conditions ($H = 0$). For aggregating units, the initial distribution reads

$$\rho(\vartheta, t = 0) = \rho_{eq}(\vartheta; H) \quad (21)$$

and the target distribution is random

$$\rho(\vartheta, t = \infty) = \rho_{eq}(\vartheta; H = 0) = \frac{1}{4\pi} \quad (22)$$

We assume linear relaxation behavior with a single relaxation time, $\tau_{rot,0}$, describing **rotation** of the aggregating units. From the theory of suspensions^[10] it follows, that rotational relaxation time for an axially symmetric, rigid particle is proportional to particle volume, v_0 , and shape factor, f , a function of the axial ratio p

$$\tau_{rot,0} \propto \frac{1}{D_{rot}} = \frac{\eta v_0}{kT} f(p) \quad (23)$$

η is effective viscosity of the medium. Applying the initial, Eq.(21), and target distribution, Eq.(22), we arrive at the transient distribution in the form

$$\rho(\vartheta, t) = \frac{1}{4\pi} + \left(\rho_{eq}(\vartheta; H) - \frac{1}{4\pi} \right) \exp \left[-\frac{t}{\tau_{rot,0}} \right] \quad (24)$$

Considering the distribution of clusters, we assume that the initial distribution is determined by thermodynamic equilibrium at $T=T_p$ and steady flow with intensity H

$$w(g, \vartheta, t = 0) = w_{eq}(g, \vartheta; T_p, H) \quad (25)$$

The target distribution at infinite time corresponds to equilibrium in quiescent conditions at $T=T_R$

$$w(g, \vartheta, t = \infty) = w_{eq,0}(g; T_R, H = 0) \quad (26)$$

The exact way in which cluster distribution changes in time is determined by Eq.(13). Like in the relaxation of single kinetic elements, we will describe the behavior of clusters with a linear relaxation equation with a single relaxation time. Relaxation of cluster distribution involves at least two different mechanisms: **rotation**, controlled by the diffusion coefficient, $D_{rot,cl}$ (relaxation time $\tau_{rot,cl}$) and **growth**, controlled by «growth diffusion» coefficient, D_{gr} (relaxation time τ_{gr}).

The first relaxation time concerns rotation of a large cluster and is proportional to cluster size, g (volume, v)

$$\tau_{\text{rot,cl}}(v) \propto \frac{1}{D_{\text{rot,cl}}(v)} = \frac{\eta v}{kT} f(p) \quad (27)$$

The other relaxation time can be derived from the nucleation theory^[1]. D_{gr} is controlled by translation of single kinetic units to, and from cluster surface. The growth diffusion coefficient, D_{gr} , increases with surface area of the cluster, and τ_{gr} decreases with 2/3 power of cluster size

$$\tau_{\text{gr}}(v) \propto \frac{1}{D_{\text{gr}}(v)} \propto \frac{\eta v^{-2/3}}{kT} \quad (28)$$

For large enough clusters, relaxation time associated with growth is much smaller than that related to rotation

$$\tau_{\text{gr}} \ll \tau_{\text{rot,cl}} \quad (29)$$

and reduces relaxation to the growth mechanism. Neglecting rotation of clusters, and making use of Eqs.(25, 26), we arrive at the time dependent cluster distribution

$$w(g, \vartheta, t) \cong w_{\text{eq},0}(g) + [w_{\text{eq}}(g, \vartheta; H) - w_{\text{eq},0}(g)] \exp\left[-\frac{t}{\tau_{\text{gr}}}\right] \quad (30)$$

Figure 7 presents reduced transient distributions of single kinetic elements and clusters. The density of clusters is taken at the point of the critical size, g^* , and orientation $\vartheta = 0$. The range of molecular orientation, $\rho(t)$, is rather narrow, but are these minor changes of ρ which control thermodynamics and kinetics of nucleation. The relaxation of critical cluster density, controlled by two different relaxation times is quite steep. Taking $\tau_{\text{rot},0}$, as a reference, we obtain different cluster relaxation rates for different $\tau_{\text{gr}}/\tau_{\text{rot},0}$ ratios. The smaller is the ratio $\tau_{\text{gr}}/\tau_{\text{rot},0}$, the faster is cluster relaxation. For the sake of simplicity, cluster size dependent τ_{gr} , is replaced with a constant, average value.

Relaxation of the transient distributions, $\rho(\vartheta)$ and $w(g, \vartheta)$, is accompanied by variation of global material characteristics. Both characteristics are controlled by the relaxation time, $\tau_{\text{rot},0}$. After the period of several relaxation times, relaxation is practically completed, and T_m and g^*

assume values corresponding to an unoriented system (respectively, $T_{m,0}$, and g_0^*). Significant orientation effects are thus concentrated in the beginning of the relaxation process, where critical cluster size is considerably reduced, and transition temperature elevated by flow orientation.

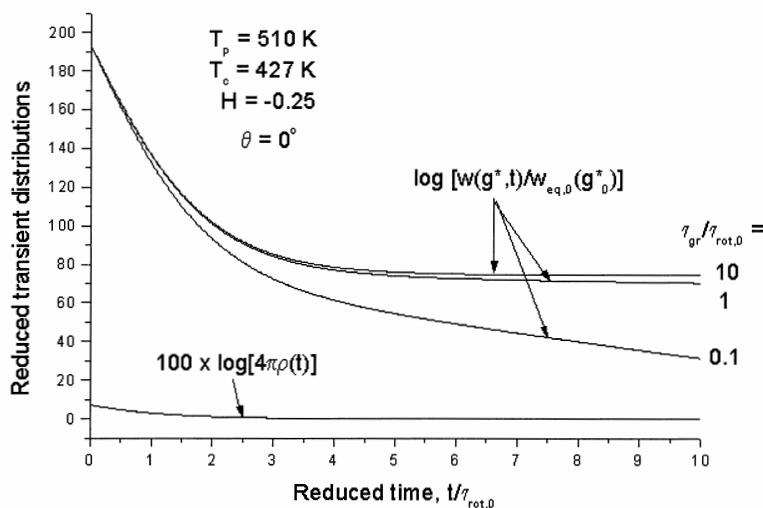


Figure 7. Reduced transient distributions of parallel oriented aggregating kinetic units, $\rho(t)$, and parallel oriented critical clusters, $w[t, g^*(t)]$, in the course of relaxation. $t_R/\tau_{rot,0}$ – time reduced by rotational relaxation time for a single aggregating unit. Relaxation time ratios, $\tau_{gr}/\tau_{rot,0}$, indicated. Calculated from Eqs.(24) and (30) for $\vartheta = 0$.

3.4. Concentration of athermal nuclei

The sample, relaxed for the period t_R in temperature T_R is rapidly transferred to subcritical temperature $T_c < T_m$, and crystallized.

There are three ways in which structure of the melt developed in flow and modified by relaxation, affects subsequent crystallization after cooling below T_m .

The first effect concerns orientation-dependent **transition temperature**, T_m . Whenever crystallization temperature, T_c , fits into the range

$$T_{m,max} \equiv T_m(\vartheta = 0) > T_c > T_m(\vartheta = \frac{\pi}{2}) \equiv T_{m,min} \quad (31)$$

the accessible range of crystal orientations is restricted from the top (ϑ_{\max}) by the condition

$$T_m(\vartheta_{\max}) = T_c \quad (32)$$

No crystals are formed when $T_c > T_{m,\max}$, and full range of orientations is accessible for $T_c < T_{m,\min}$.

The second effect is related to **critical cluster size**, g^* . Like critical transition temperature, critical cluster size depends on orientation of the aggregating kinetic units. Perpendicular crystals ($\vartheta \approx \pi/2$) require deep undercooling, large cluster sizes, and their production is negligible compared to that of parallel ones.

The third effect results from **transient cluster distribution**, $w(g, \vartheta, t)$. The number of stable clusters capable of growing in the temperature T_c , is described by the integral of cluster density over cluster sizes from the critical limit, g^* , to infinity (Eqs. 14, 18). Thermo-mechanical history of the system (flow, relaxation) affects both, lower integration limit (g^*) and the kernel function, $w(g)$. In an oriented system, relaxation reduces density of oriented clusters, and concentration of parallel oriented athermal nuclei. In contrast to that, the density of perpendicular clusters ($\vartheta = \pi/2$) increases in time, leading to slightly higher (though still negligible) concentration of nuclei (and crystals).

Using transient cluster distribution from Eq.(30), Equation (18) can be presented in the form

$$\Delta N_{\text{ath}}(t_R) = \Delta N_{\infty}(t_R) + [\Delta N_0(t_R) - \Delta N_{\infty}(t_R)] \exp\left[-\frac{t_R}{\tau_{gr}}\right] \quad (33)$$

where

$$\Delta N_{\infty}(t_R) = 2\pi N_{\text{tot}} \int_0^{\delta\vartheta} \sin\vartheta \, d\vartheta \int_{g^*(\vartheta, T_c, t_R)}^{\infty} w_{\text{eq},0}(g; T_p) \, dg \quad (34)$$

$$\Delta N_0(t_R; H) = 2\pi N_{\text{tot}} \int_0^{\delta\vartheta} \sin\vartheta \, d\vartheta \int_{g^*(\vartheta, T_c, t_R)}^{\infty} w_{\text{eq}}(g, \vartheta; T_p, H) \, dg \quad (35)$$

are integrals taken over the initial (flow induced) and final (completely relaxed) cluster

distributions. ΔN_0 and ΔN_∞ are not independent of time, however, because the lower integration limit, g^* , depends on transient orientation distribution, $\rho(\vartheta, t)$, controlled by rotational relaxation time, $\tau_{\text{rot},0}$. Consequently, the effective number of athermal nuclei depends on two different relaxation times one related to rotational ($\tau_{\text{rot},0}$) another one to translational motions of the aggregating units (τ_{gr}).

Figures 8 and 9 show reduced concentrations of oriented athermal nuclei as functions of flow intensity, H , and relaxation period, t_R . Values, reduced by asymptotic concentration of athermal nuclei in an unoriented system, $\Delta N_{\text{ath},\text{eq}0}$, were used, to eliminate the ill defined normalization factor, N_{tot} . It is evident that ΔN_{ath} strongly increases with flow intensity (Figure 8) and relaxes to negligible levels after less than one relaxation time (Figure 9). Flow effects, evident at short relaxation periods, consist in a dramatic increase of the concentration of athermal nuclei (parallel to flow direction). The orientation effects are sensitive to flow intensity, H (Figure 8) and gradually disappear in time (Figure 9).

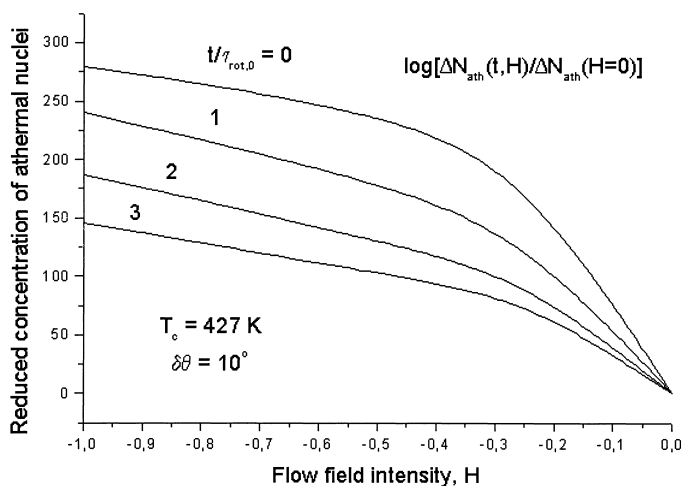


Figure 8. Reduced concentration of oriented athermal nuclei, $\Delta N_{\text{ath}}(t_R; H) / \Delta N_{\text{ath}}(t = \infty)$, as a function of flow field intensity, H , prior to relaxation. Relaxation periods, $t_R / \tau_{\text{rot},0}$ indicated. $\tau_{\text{gr}} / \tau_{\text{rot},0} = 1$. Flow and relaxation temperatures: $T_p = T_R = 510$ K for $H = 0$ and $H = -0.25$; 540 K for $H = -0.5$ and 600 K for $H = -1$. Integrated orientation range, $\delta\vartheta = 10^\circ$. Calculated from Eqs.(33-35).

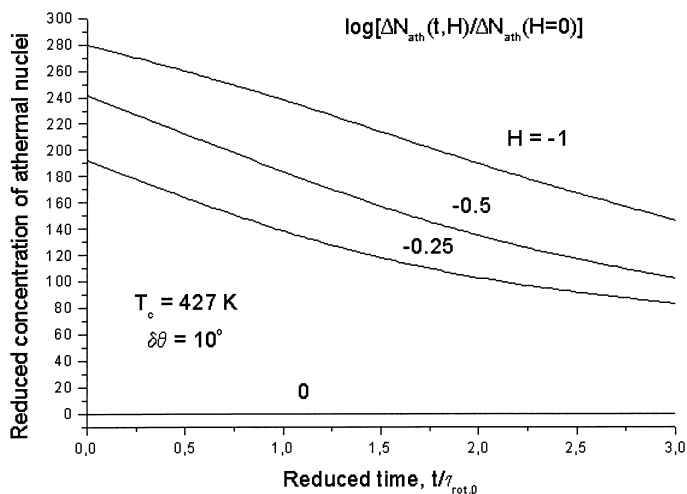


Figure 9. Reduced concentration of oriented athermal nuclei, $\Delta N_{\text{ath}}(t; H) / \Delta N_{\text{ath}}(t = \infty)$, as a function of reduced relaxation period, $t_R / \tau_{\text{rot},0}$. Field intensity prior to relaxation, H , indicated. $\tau_{\text{gr}} / \tau_{\text{rot},0} = 1$. Integrated orientation range, $\delta\theta = 10^\circ$. Calculated from Eqs.(33-35). Flow and relaxation temperatures, see Figure 8.

4. Microscopy experiments

Morphology is an extremely sensitive indicator of crystallization taking place in an oriented polymer system. Already at small levels of orientation, well before development of fibrillar superstructures sets in, nucleation density is strongly enhanced. The fiber pulling experiment described in References 4-7 mimics, **in a shear flow**, the orientation-relaxation-crystallization processes discussed in Section 3. Under these conditions it can be directly observed that application of the flow field produces a remarkable increase of nucleation density and it is responsible for the development of cylindritic (transcrystalline) morphology all around the pulled fiber^[5,6]. However, if the system is kept in the molten state long enough to relax the perturbations due to flow, a uniform spherulitic morphology is detected throughout the whole sample. In this section we provide an illustrative example obtained by performing the experiments with a high molecular weight isotactic polybutene-1 sample ($M_w = 700,000$; $M_n = 100,000$) purchased from Aldrich.

A single glass fiber ($\phi = 20 \mu\text{m}$), imbedded in the mid-plane of a $200 \mu\text{m}$ thick film confined between two cover glasses, is pulled along its axis at a linear rate of a few mm/s through the

molten polymer at a temperature $T_p > T_m$ ($T_p = 145^\circ\text{C}$) in a Mettler Hot stage. In these conditions a shear rate of the order of several hundreds reciprocal seconds establishes at the fiber-melt interface^[4]. Immediately after pulling the sandwich is quickly transferred to a second hot stage, set at a suitable relaxation temperature, $T_R = 150^\circ\text{C}$, where it is hold to relax during various times, t_R , before its transfer to a final stage at which crystallization takes place in isothermal conditions, $T_c = 90^\circ\text{C}$.

Micrographs of polybutene-1 crystallized after various flow and temperature histories indicate some important features^[11]:

- nucleation is strongly enhanced by flow and crystalline structures mainly develop from the fiber surface, where the most intense shear flow field was acting during the pulling stage^[4]. Due to mutual hindrance of closely spaced nuclei on fiber surface, the growth of crystalline entities can only take place in the direction perpendicular to fiber axis.
- the average distance between crystalline structures monotonically increases with time and temperature of relaxation (t_R , T_R). Eventually, after sufficient long relaxation, the spherulitic morphology characteristic of crystallization in quiescent conditions is restored.
- the holding time needed to fully erase memory of flow on subsequent crystallization increases with decreasing T_R and it is strongly temperature dependent.

Some of these features are evident in Figure 10. Qualitatively similar results have been obtained from experiments performed on PEO and *i*-PP^[6], and also on *i*-PS and will be comprehensively discussed elsewhere^[11]; this indicates that the above features are representative of the general behavior of all crystallizable polymers.

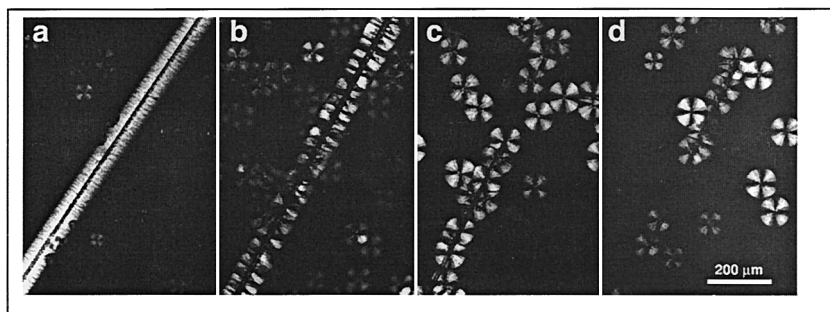


Figure 10. Microscopic photographs of high-molecular-weight polybutene-1 subjected to shear flow orientation ($T_p = 145^\circ\text{C}$), relaxation ($T_R = 150^\circ\text{C}$) and crystallization ($T_c = 90^\circ\text{C}$)¹¹. Relaxation periods, t_R : a) 20 sec., b) 30 sec., c) 40 sec., d) 60 sec.

Image analysis, performed by means of *Image Pro Plus* package, on micrographs similar to

those shown in Figure 10 enabled us to obtain a semi-quantitative estimate of linear density of nuclei along the fiber axis.

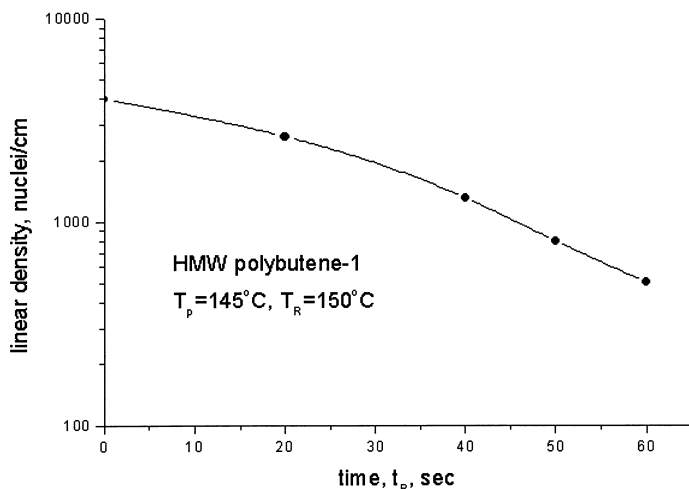


Figure 11. Linear density of nuclei in high-molecular-weight polybutene-1 subjected to flow orientation, relaxation, and crystallization vs. relaxation period. Conditions, see Figure 10^[11].

It seems reasonable to interpret the inverse of inter-spherulitic distance as a **linear density of nuclei**. Monotonical change of this density with time of heating of the sample in quiescent conditions, t_R (Figure 11) confirms relaxational mechanism of this phenomenon and is qualitatively consistent with predictions of the model (see Figure 9). For sake of comparison, the inverse average distance between nuclei measured in a quiescent crystallization experiment, performed on the same material and at the same crystallization temperature of 90°C, is of the order of 100-120 μm . This corresponds to a linear nucleation density of about 80-100 nuclei/cm, a value that is close to the asymptotic limit estimated from the relaxation curve of Figure 11.

The fact that flow induced **orientation and relaxation in the melt** ($T_p > T_m$, $T_R > T_m$) controls crystallization in a supercooled system ($T_c < T_m$) strongly points to an **athermal mechanism of nucleation**. Unstable molecular clusters, formed in an oriented system and partially restructured in the relaxation step **are converted** into stable **athermal nuclei** when the

system is cooled down to crystallization temperature.

5. Conclusions

In systems oriented by flow, nucleation (and crystallization), becomes *selective with respect to orientation*. Critical transition temperature, T_m , nucleation and crystallization rates are elevated above the level characteristic for an unoriented system for clusters oriented along the flow axis ($\vartheta = 0$), and suppressed for perpendicular clusters ($\vartheta = \pi/2$). Therefore, nucleation (and, consequently, crystallization) is practically confined to a narrow range of orientations around the flow axis. The effect, controlled by thermodynamic and kinetic factors is typical for aggregation of orientable kinetic units.

The nature of *flow-induced memory* consists in formation in melt oriented, thermodynamically unstable clusters, convertible to stable nuclei on cooling below T_m . Such a mechanism is known as *athermal nucleation*. The concentration of clusters depends on flow conditions (temperature, flow intensity). Heating of the melt in the absence of flow leads to partial relaxation of cluster distribution and reduction of the number of potential nuclei.

Microscopic experiments are qualitatively consistent with the simple model developed in this paper. The model explains the nature of the phenomenon, but it is unable to reproduce quantitatively the experimental data. Both, extension of the theoretical model, and new measurements are desired.

Acknowledgements

The authors duly acknowledge that the cooperation on the above topics started thanks to the COST P1 Action of European Community (WG on Polymer Crystallization)

- [1] A. Ziabicki, *J. Chem. Phys.* **1986**, 85, 3042.
- [2] A. Ziabicki, G. C. Alfonso, *Colloid & Polymer Sci.* **1994**, 272, 1027.
- [3] G. C. Alfonso, A. Ziabicki, *Colloid & Polymer Sci.*, **1995**, 273, 317.
- [4] B. Monasse, *J. Mater. Sci.* **1992**, 27, 6047.
- [5] J. Varga, J. Karger-Kocsis, *J. Polym. Sci. Part B: Polym. Phys.* **1996**, 34, 657.
- [6] G. C. Alfonso, P. Scardigli, *Macromol. Symposia* **1997**, 118, 323.
- [7] P. Sajkiewicz, A. Wasiak, D. Kukla, M. Boguszewski, *J. Mater. Sci. Lett.* **2000**, 19, 847.
- [8] A. Ziabicki, *Arch. Mech.* **1991**, 43, 57.
- [9] A. Ziabicki, *J. Chem. Phys.* **1977**, 66, 1638.
- [10] G.B. Jeffery, *Proc. Roy. Soc. (London)* **1922**, A102, 161. See also: M. Doi, S. F. Edwards, *The Theory of Polymer Dynamics*, Clarendon Press, Oxford 1986.
- [11] G. C. Alfonso, F. Azzurri, in preparation